SEISMIC RESPONSE OF TALL BUILDINGS COUPLED WITH ROCKING WALLS

M. Aghagholizadeh[(1)] and N. Makris[(2)]

[(1)] Lecturer, Department of Civil and Environmental Engineering, Southern Methodist University, Texas, USA, mehrdadag@smu.edu

[(2)] Professor,Department of Civil and Environmental Engineering, Southern Methodist University, Texas, USA, nmakris@smu.edu

Abstract

This paper investigates the inelastic response of a yielding structure coupled with a damped rocking wall. The paper first derives the nonlinear equations of motion of a yielding oscillator coupled with a rocking wall when it is equipped with vertical energy dissipation devices, which offer either hysteretic or viscous damping. Then, the dependability of the one-degree of freedom idealization is validated against the nonlinear time-history response analysis of a multistory moment-resisting frame that is coupled with a damped stepping rocking wall. The SDOF idealization presented in this paper compares satisfactory with finite-element analysis of a multi-story building coupled with a damped stepping rocking wall; therefore, the SDOF idealization can be used with confidence for preliminary analysis and design. The study also shows that in most cases, use of dampers are effective way of reducing maximum deformation in the coupled system; while the additional lever arm for the dampers appears to have marginal effect on the peak response, in particular for taller walls.

Keywords: shear wall; earthquake engineering; seismic protection; rocking; recentering

1. Introduction

The concept of coupling the lateral response of a moment resisting frame with a rigid core system goes back to the early work of Paulay and Fintel [1, 2]. With this design, interstory drift demands are reduced at the response of transferring appreciable shear-forces and bending moments at the foundation of the rigid core wall.

About the same time, the early concepts of the alternative strategy for seismic protection by modifying the response of a structure with specially designed supplemental devices were brought forward in the seminal papers by Kelly et al. [3].

Clearly, the paper by Kelly et al.[3] marks the beginning of the use of response modification devices for the seismic protection of structures and among several original contributions it suggests the use of rocking shear-walls in association with energy dissipation devices for the seismic protection of moment-resisting frames (Fig. 2 of the paper by Kelly et al. [3] that is reproduced in this paper as Fig. 1 (a)). In this way, the stepping core wall does not suffer from large ductility demands and possible cyclic degradation while recentering happens invariably due to gravity. Despite its remarkable originality and technical merit, the paper by Kelly et al. 1972 did not receive the attention it deserved and it was some two decades later that the PRESSS Program reintroduced the concept of uplifting and rocking of the joint shear wall system [4–6].

Following the PRESSS program a number of publications presented experimental and analytical studies on the cyclic loading of structural systems coupled with vertically restrained rocking walls [7, 8]. Given that damping during impact as the wall alternate pivot points is low ([9–11] and references reported therein), the idea of introducing supplemental energy dissipation devices in structural systems coupled with rocking walls received revived attention ([12–15] among others.) some 30 years after the original idea presented by Kelly et al. [3] . These subsequent studies were partly motivated from the need to eliminate the generation of a weak-story failure in multi-story buildings together with the need to ensure recentering of the yielding frame [16–18]. At the same time alternative proposals on the use of pinned rocking walls [19, 20], where the weight of the wall works against the stability of the structure motivated a series of recent studies that revisited the dynamics of a moment-resisting frame coupled with a rocking wall either stepping or pinned [21–24] by accounting explicitly of the role of the of the rotational inertia of the rocking wall. These studies led to valuable conclusions, including that the vertical tendons in tall, stiff, stepping rocking walls have marginal contribution even when they offer a high axial stiffness [24].

In view of these recent findings, the paper examines the contribution of viscous and hysteretic dampers to the response of a yielding frame coupled with a rocking wall shown in Fig 1.

2. Dynamics of a Yielding Oscillator Coupled with a Rocking Wall with Supplemental Damping

With reference to Fig. 1(b), this study examines the dynamic response of a yielding single-degree-of-freedom (SDOF) structure, with mass, m_s, pre-yielding stiffness, k_1, post-yielding stiffness, k_2 and strength, Q, that is coupled with a free-standing stepping rocking wall of size, $R = \sqrt{b^2 + h^2}$, slenderness, $\tan\alpha = b/h$, mass m_w and moment of inertia about the pivoting (stepping) points O and O', $I = \frac{4}{3} m_w R^2$. Vertical energy dissipation devices are mounted to the rocking wall at a distance, d, from the pivoting points of the wall as shown in Figs. 1(b) and 2. In the interest of simplicity, it is assumed that the arm with length L, that couples the motion is articulated at the center mass of the rocking wall at a height, h from its foundation as shown in Fig. 1(b).

2.1. Kinematics of the Structural System

During rocking motion, the center of mass of the rocking wall uplifts by v; therefore, the initially horizontal coupling arm rotates by an angle ψ. Accordingly, the horizontal translation of the center of mass of the rotating wall, x, is related to the horizontal displacement of the SDOF oscillator, u, via the expression, $\cos\psi = 1 - \frac{u-x}{L}$; whereas, $\sin\psi = v/L$. From the identity, $\cos^2\psi + \sin^2\psi = 1$, one concludes that the horizontal displacement,

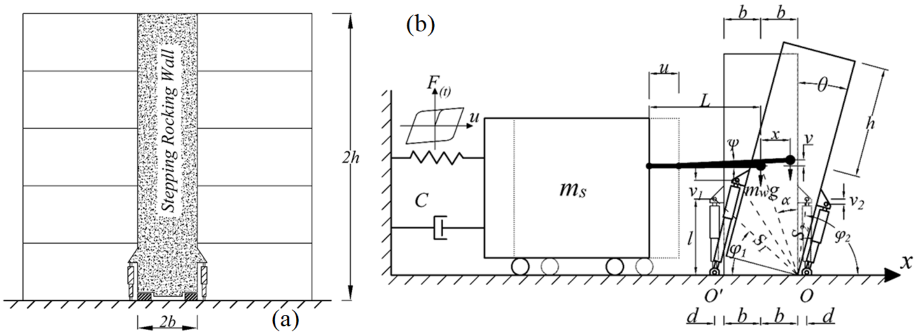

Fig. 1 – (a) Moment-resisting frame coupled with a stepping rocking wall with vertical supplemental dampers as was introduced by Kelly, et al. [3], (b) A single-degree-of-freedom idealization of a yielding oscillator coupled with a stepping rocking wall with supplemental dampers.

u of the SDOF oscillator is related to the horizontal displacement x of the center of mass of the rotating wall via the expression:

$$\frac{u}{L} = 1 + \frac{x}{L} - \sqrt{1 - \frac{v^2}{L^2}} \tag{1}$$

In this paper, the coupling arm is assumed to be long enough so that v^2/L^2 is much smaller that unity ($v^2/L^2 << 1$); and in this case $u = x$. A recent study by Makris and Aghagholizadeh [21] on the response of an elastic oscillator coupled with a rocking wall showed that the effect due to a shorter coupling arm is negligible.

The system under consideration is a single-degree-of-freedom system where the lateral translation of the mass, u is related to the rotation of the stepping rocking wall θ via the expression (In equations of this paper, whenever there is a double sign (e.g. $\pm$) the top sign is for $\theta > 0$ and the bottom sign is for $\theta < 0$):

$$u = \pm R\left[\sin\alpha - \sin(\alpha \mp \theta)\right], \quad \dot{u} = R\dot{\theta}\cos(\alpha \mp \theta) \; and \quad \ddot{u} = R\left[\ddot{\theta}\cos(\alpha \mp \theta) \pm \dot{\theta}^2 \sin(\alpha \mp \theta)\right] \tag{2}$$

During rocking motion of the wall, the upward displacement; v_1 of the damper appended at the side of the wall across the pivoting point is

$$v_1 = S_1[\sin(\phi_1 \pm \theta) - \sin\phi_1] \tag{3}$$

whereas the downward displacement; v_2 of the damper appended at the side of the wall that is stepping on the pivoting point is

$$v_2 = S_2[\sin\phi_2 - \sin(\phi_2 \mp \theta)] \tag{4}$$

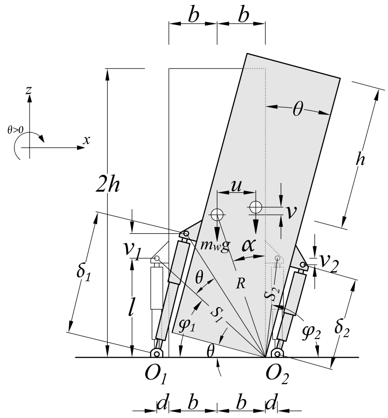

Fig. 2 – Geometric quantities pertinent to the dynamic analysis of a rocking wall with energy dissipators.

where $S_1 = \sqrt{(2b+d)^2 + l^2}$, $S_2 = \sqrt{d^2 + l^2}$, $sin\phi_1 = l/S_1$ and $\sin\phi_2 = l/S_2$.
The elongation of damper, e_1 appended at the side of the column across the pivoting point is: $e_1 = \delta_1 - l$, where δ_1 is offered by the cosine rule:

$$\delta_1 = S_1\sqrt{1 + \cos^2\varphi_1 - 2\cos\varphi_1\cos(\varphi_1 \pm \theta)} \tag{5}$$

and by using that $e_1 = \delta_1 - l$, the elongation of the damper is

$$e_1(t) = S_1\left[\sqrt{1 + \cos^2\varphi_1 - 2\cos\varphi_1\cos(\varphi_1 \pm \theta)} - \sin\varphi_1\right] \tag{6}$$

The time derivative of the elongation $e_1(t)$ is expressed in terms of the independent variable θ and its time derivative, $\dot{\theta}$:

$$\dot{e}_1(t) = \frac{S_1\cos\varphi_1\,\dot{\theta}\sin(\varphi_1 \pm \theta)}{\sqrt{1 + \cos^2\varphi_1 - 2\cos\varphi_1\cos(\varphi_1 \pm \theta)}} \tag{7}$$

Similarly, the contraction of the dampers appended at the side of the column that is stepping on the pivoting point is $e_2 = l - \delta_2$, where δ_2 is

$$\delta_2 = S_2\sqrt{1 + \cos^2\varphi_2 - 2\cos\varphi_2\cos(\varphi_2 \mp \theta)} \tag{8}$$

and by using that $e_2 = l - \delta_2$, the contraction of the damper is

$$e_2(t) = S_2\left[\sin\varphi_2 - \sqrt{1 + \cos^2\varphi_2 - 2\cos\varphi_2\cos(\varphi_2 \mp \theta)}\right] \tag{9}$$

The time derivative of the contraction $e_2(t)$ is expressed in terms of the independent variable θ and its time derivative, $\dot{\theta}$

$$\dot{e}_2(t) = \frac{S_2\cos\varphi_2\dot{\theta}\sin(\varphi_2 \mp \theta)}{\sqrt{1 + \cos^2\varphi_2 - 2\cos\varphi_2\cos(\varphi_2 \mp \theta)}} \tag{10}$$

2.2. Constitutive Laws of Non-Linear Viscous and Hysteretic Dissipation Devices

The energy dissipation devices appended to the rocking column as shown in Fig. 1 can be either linear or nonlinear fluid dampers [25, 26] or hysteretic (yielding) dampers such as buckling restrained braces [27–30].

$$F_d = C_q\,|\dot{e}(t)|^q \text{sgn}\,[\dot{e}(t)] \tag{11}$$

where $0 < q < 1$ is the exponent of the damper, C_q is the damping constant with units: $[m][L]^{1-q}[T]^{q-2}$, and $sgn[\,]$ is the signum function. e(t) is the stroke of the damper that is given by Eq. (4) when the damper is in elongation ($e(t) = e_1(t)$) and by Eq. (7) when the damper is in contraction ($e(t) = e_2(t)$). When $q = 1$, Eq. (9) reduces to a linear viscous law: $F_d = c_1\dot{e}(t)$.

When torsionally yielding steel-beam dampers, buckling restrained braces (BRB) or other yielding devices are used, their constitutive law can be expressed by the Bouc-Wen model [31, 32]

$$F_d = ak_d\,e(t) + (1-a)k_d\,u_y\,z(t) \tag{12}$$

in which, k_d is the preyielding stiffness of the device, u_y is the yield displacement, a is the post-to-pre- yielding stiffness ratio and $-1 \le z(t) \le 1$ is the dimensionless internal variable described by

$$\dot{z}(t) = \frac{1}{u_y}\left[\dot{e}(t) - \beta\dot{e}(t)\,|z(t)|^n - \gamma\,|\dot{e}(t)|\;z(t)\,|z(t)|^{n-1}\right] \tag{13}$$

Again, $e(t)$ is the stroke of the hysteretic device that is given by Eq. (4) when the damper is in elongation ($e(t) = e_1(t)$) and by Eq. (7) when the damper is in contraction ($e(t) = e_2(t)$). In Eq. (15), constants β, γ and n are model parameters to be discussed later in the paper.

2.3. Equation of Motion of the Entire System

With reference to Fig. 1(b) dynamic equilibrium of the mass m_s gives:

$$m_s(\ddot{u} + \ddot{u}_g) = -F_s - c\dot{u} + T \tag{14}$$

where F_s is the force the develops in the nonlinear spring and is described by the Bouc-Wen model [31, 32].

$$F_s(t) = ak_1u(t) + (1-a)k_1u_yz(t) \tag{15}$$

in which, $a = k_2/k_1$ is the post-to-pre- yielding stiffness ration of the nonlinear oscillator and $-1 \le z(t) \le 1$ is a dimensionless internal variable described similarly with Eq. (15) but with constants β, γ and n defined based on oscillator hysteretic behavior.

Case 1. $\theta > 0$:

For positive rotations ($\theta > 0$), dynamic equilibrium of the rotating wall with mass, m_w, equipped with vertical dampers installed on each of its side as shown in Figs. 1(b) and 2 gives

$$I\ddot{\theta} = -TR\cos(\alpha-\theta) - m_wgR\sin(\alpha-\theta) - m_w\ddot{u}_gR\cos(\alpha-\theta) - F_{d_1}r_1 - F_{d_2}r_2 \tag{16}$$

in which $F_{d_1}$and F_{d_2} are the damping forces in the damper across the pivoting point and the damper at the pivoting point side respectively and r_1 and r_2 are moment arms of the dampers about pivoting point

$$r_1 = S_1\cos\varphi_1 \frac{\sin(\varphi_1 \pm \theta)}{\sqrt{1+\cos^2\varphi_1 - 2\cos\varphi_1\cos(\varphi_1 \pm \theta)}} \tag{17}$$

$$r_2 = S_2\cos\varphi_2 \frac{\sin(\varphi_2 \mp \theta)}{\sqrt{1+\cos^2\varphi_2 - 2\cos\varphi_2\cos(\varphi_2 \mp \theta)}} \tag{18}$$

The axial force T appearing in Eq. 16 is replaced with the help of Eqs. 14 and 15, whereas for a rectangular stepping wall, $I = 4/3m_wR^2$ and upon dividing with m_wR^2, Eq. 16 gives the following equation which is expressed only in terms of the variable, $\theta(t)$.

$$\begin{aligned}&\left(\tfrac{4}{3} + \sigma\cos^2(\alpha-\theta)\right)\ddot{\theta} + \sigma\cos(\alpha-\theta)\left[a\omega_1^2(\sin\alpha - \sin(\alpha-\theta)) + 2\xi\omega_1\dot{\theta}\cos(\alpha-\theta)\right.\\ &\left.+\dot{\theta}^2\sin(\alpha-\theta) + (1-a)\omega_1^2\tfrac{u_y}{R}z(t)\right]\\ &= -\tfrac{g}{R}\left[(\sigma+1)\tfrac{\ddot{u}_g}{g}\cos(\alpha-\theta) + \sin(\alpha-\theta) + \tfrac{F_{d_1}}{m_wg}\tfrac{r_1}{R} + \tfrac{F_{d_2}}{m_wg}\tfrac{r_2}{R}\right]\end{aligned} \tag{19}$$

in which $\sigma = m_s/m_w$ is the mass ratio parameter.

Case 2. $\theta < 0$:

For negative rotations one can follow the same reasoning and the equation of the coupled system is:

$$\begin{aligned}&\left(\tfrac{4}{3} + \sigma\cos^2(\alpha+\theta)\right)\ddot{\theta} - \sigma\cos(\alpha+\theta)\left[a\omega_1^2(\sin\alpha - \sin(\alpha+\theta)) - 2\xi\omega_1\dot{\theta}\cos(\alpha+\theta)\right.\\ &\left.+\dot{\theta}^2\sin(\alpha+\theta) - (1-a)\omega_1^2\tfrac{u_y}{R}z(t)\right]\\ &= -\tfrac{g}{R}\left[(\sigma+1)\tfrac{\ddot{u}_g}{g}\cos(\alpha+\theta) - \sin(\alpha+\theta) + \tfrac{F_{d_1}}{m_wg}\tfrac{r_1}{R} + \tfrac{F_{d_2}}{m_wg}\tfrac{r_2}{R}\right]\end{aligned} \tag{20}$$

In Eqs. (19) and (20), the terms multiplied with the parameter $\sigma = m_s/m_w$ are associated with the dynamics of the nonlinear oscillator whereas the remaining terms are associated with the dynamics of the rocking wall with vertical dampers. When the yielding oscillator is absent ($\sigma = \omega_1 = \xi = 0$), Eqs. (19) and (20) reduce to the equations of motion of the free-standing rocking wall equipped with dampers [33].

3. Parameters of the Problem

The Bouc-Wen model described by Eqs. (15) and (13) is a phenomenological model of hysteresis originally proposed by Bouc [31] and subsequently generalized by Wen [32]. The Bouc-Wen model essentially builds on the bilinear idealization shown in the bottom-left of Fig. 1. Only three of the five constitutive parameters (k_1= pre-yielding stiffness, k_2= post-yielding stiffness, u_y= yield displacement, Q= strength and F_y= yielding force) of the bilinear Bouc-Wen model are independent and needed to be defined.

In this work, the authors select the pre-yielding stiffness $k_1 = m_s\omega_1^2$, the post-yielding stiffness $k_2 = ak_1$ and the strength of the structure Q. With reference to Fig. 1 (bottom-left), $F_y = k_1 u_y = Q + k_2 u_y$. Accordingly, $u_y = Q/(k_1 - k_2)$ and $F_y = k_1 Q/(k_1 - k_2)$. The parameters β, γ and n appearing in Eq. (13) are established from past studies on the parameter identification of yielding concrete structures and assume the values: $\beta = 0.95$, $\gamma = 0.05$ and $n = 2$ [34, 35]. With the parameters $\beta = 0.95$, $\gamma = 0.05$ and $n = 2$ being established, the peak inelastic displacement, u_{max} of the SDOF system shown in the Fig. 1 (bottom) is a function of the following parameters:

$$u_{max} = f(\omega_1, \frac{Q}{m_s}, a, \xi, p, \tan\alpha, \sigma, g, F_d, parameters\ of\ excitation) \tag{21}$$

Here, it is assumed that upon yielding, the structure maintains a mild, positive, post-yielding stiffness = $k_2 = 0.05k_1$, therefore $a = 0.05$ [34, 35]. Furthermore, it is assumed that the pre-yielding damping ratio, $\xi = C/(2m_s\omega_1) = 0.03$ and rocking walls with slenderness, $\tan\alpha = 1/6$.

In this study, torsionally yielding steel-beam damper similar to one that has been used in the stepping pier of the South Rangitikei Rail Bridge in New Zealand is used [3, 36, 37], hence hysteretic dampers with $k_d \cdot u_y = 900kN = \frac{k_d u_y}{m_w g} = 0.05$ is selected.

First, zero-length dampers attached at the pivoting points are considered ($l = \phi_1 = \phi_2 = d = S_2 = 0$ and $S_1 = 2b$); therefore Eqs. (6) and (17) simplify to

$$e_1 = 2\sqrt{2}b\sqrt{1-\cos\theta} \qquad and \qquad r_1 = \sqrt{2}\frac{b\sin\theta}{\sqrt{1-\cos\theta}} \tag{22}$$

For small rotations $\cos\theta = 1 - \theta^2/2$ and $\sin\theta = \tan\theta = \theta$, therefore, the expressions given by Eq. (22) further simplify to

$$e_1 = 2b\tan\theta \qquad and \qquad r_1 = 2b\frac{\sin\theta}{\theta} \approx 2b \tag{23}$$

Accordingly, the full nonlinear equation of the stepping pier with zero-length hysteretic dampers at its pivoting points can be found by plugging in values of F_{d_1} from Eqs. (11) or (12), r_1 from Eq. (23) and $F_{d_2} = r_2 = 0$ into equations of motion (19) and (20).

In the similar case, when zero-length viscous dampers are used at the pivoting points, the time derivative of the stroke is

$$\dot{e}_1 = \sqrt{2}b\dot{\theta}\sqrt{1+\cos\theta} \tag{24}$$

which for small rotations simplifies to $\dot{e}_1(t) = 2b\dot{\theta}$.

By comparing, the right hand-side of the equation of motion for each cases of hysteretic and viscous damper, a peak damping force from the viscous dampers $C_q[2b\dot{\theta}_{max}]^q$, will match the yield capacity of the torsionally yielding hysteretic dampers when

$$C_q = \frac{k_d u_y}{(2b\dot{\theta}_{\max})^q} \tag{25}$$

which for the case of a linear viscous damper Eq. (25) simplifies to

$$C = \frac{k_d u_y}{2b\dot{\theta}_{\max}} \tag{26}$$

Fig. 3 plots force-displacement loops, together with displacement $u(t)$, normalized velocity $\dot{\theta}/p$, time histories with a structure having $T_1 = 0.8sec$, $Q/m_s = 0.15g$ which is coupled with a rocking wall $\omega_1/p = 10$, $\sigma = m_s/m_w = 5$ with supplemental hysteretic dampers (left) and linear viscous dampers (right) when subjected to the Newhall/360 ground motion recorded during 1994 Northridge, California earthquake.

To have comparable damping forces for hysteretic damper and linear-viscous damper (considering hysteretic damping force ratio of $\frac{k_d u_y}{m_w g} = 0.05.$), using Eq. (26), damping constant C_1 of the viscous damper calculated as $C_1 = 479\ Mg/sec$, since the maximum rotational velocity for this case is $\dot{\theta}_{max} = 0.058\ rad/sec$ which yields to a similar damping force for both cases.

Fig. 3 in both cases shows that the rocking wall suppress the maximum response and use of dampers plays in favor of reducing the peak displacements. In Fig. 3 (bottom) force-deformation relations of hysteretic (left) and viscous (right) is shown. The loops at the bottom show left leg damper (heavier line) when the wall is rotating on right corner and right leg damper when the wall is on left pivoting point. It should be noted that

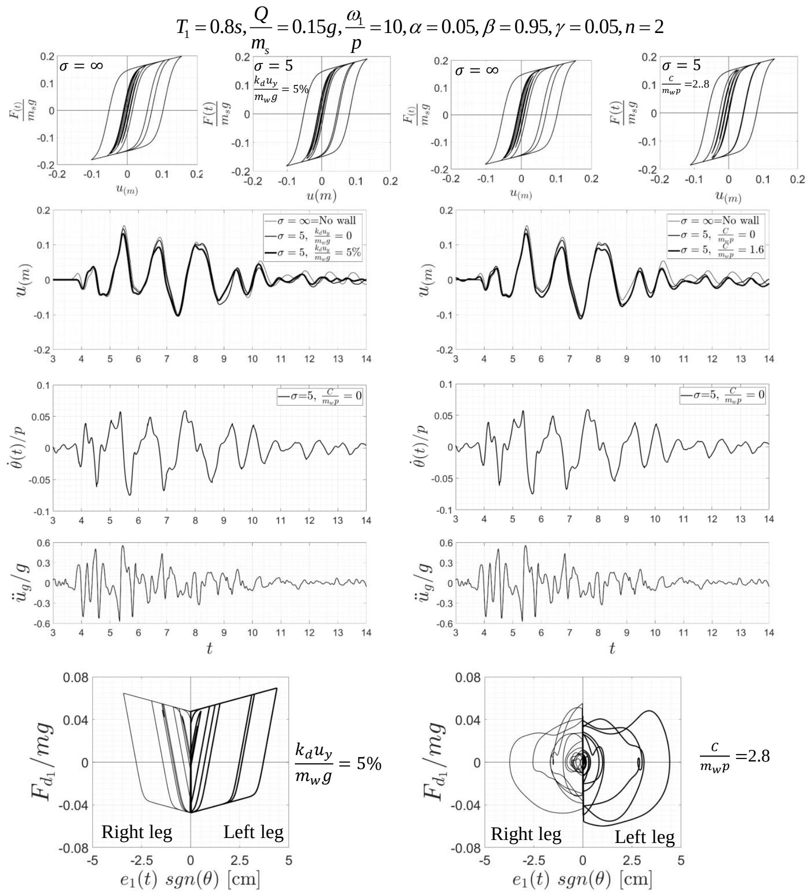

Fig. 3 – Time history analysis of a nonlinear SDOF oscillator coupled with a damped stepping rocking wall, when subjected to the Newhall/360 ground motion recorded during the 1994 Northridge, California earthquake. Thin lines: No wall, Heavy solid lines: (thinner) with wall and no dampers (heavier) wall with hysteretic (left) and linear viscous (right) zero-length dampers. Bottom: Force-displacement loops of the dampers.

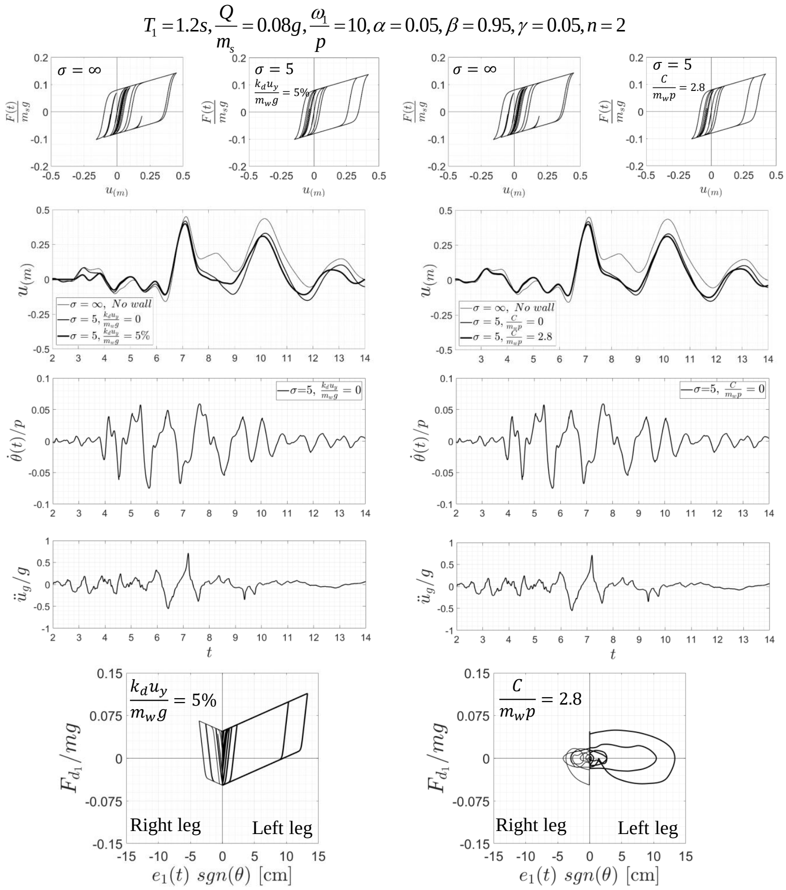

Fig. 4 – Time history analysis of a nonlinear SDOF oscillator coupled with a damped stepping rocking wall, when subjected to the REHS ground motion recorded during the 2011 Christchurch, New Zealand earthquake. Thin lines: No wall, Heavy solid lines: (thinner) with wall and no dampers (heavier) wall with hysteretic (left) and linear viscous (right) zero-length dampers. Bottom: Force-displacement loops of the dampers.

since the dampers are at the pivoting point they will work only when they are appended at the side of the wall across the pivoting point.

Fig. 4 plots force-displacement loops, together with displacement $u(t)$ time histories with a structure having $T_1 = 1.2sec$, $Q/m_s = 0.08g$ which is coupled with a rocking wall $\omega_1/P = 10$, $\sigma = m_s/m_w = 5$ with supplemental hysteretic dampers (left) and linear viscous dampers (right) when subjected to the REHS ground motion recorded during 2011 Christchurch, New Zealand earthquake. Similar to the results presented in Fig. 3, Fig. 4 shows that the damped system has smaller maximum deformation and the coupled system has minimal residual deformation. In this case since the maximum rotational velocity is $\dot{\theta}_{max} = 0.038$, viscous damping constant C_1 (calculated from Eq. (26)) is equal to $C_1 = 1700\ Mg/sec$.

4. Validation of The SDOF–Idealization

In this section the dependability of the single-degree-of-freedom idealization shown in Fig. 1 is examined against the results obtained with the open-source code OpenSees when analyzing the nine-story moment resisting steel structure designed for the SAC Phase II Project [38]. This structure that is well-known to the literature [39, 40] was designed to meet the seismic code (pre-Northridge Earthquake) and represents typical

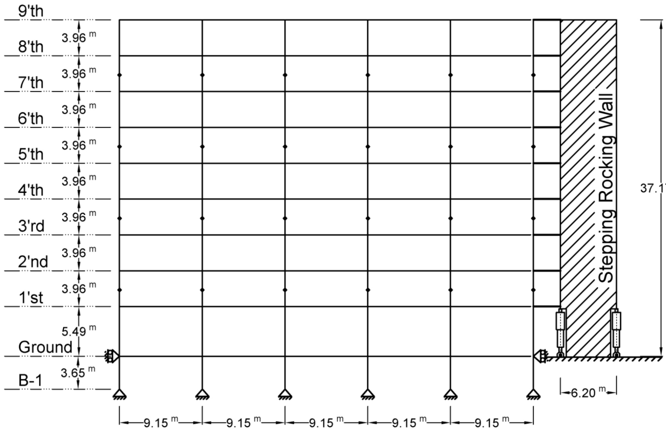

Geometric and Physical Characteristics			
Beams [248 MPa]		Columns [345 MPa]	
• Ground-2nd level	W36x160	• B1-1st level	W14x500
• 3rd-6th level	W36x135	• 1st-3rd level	W14x455
• 7th level	W30x99	• 3rd-5th level	W14x370
• 8th level	W27x84	• 5th-7th level	W14x283
• 9th level	W24x68	• 7th-9th level	W14x257
Columns • Column sizes change at splices and they are marked on the figure.			
Seismic mass : • Ground level $9.5 \times 10^5\ kg$ • 1st level $1.0 \times 10^6\ kg$ • 2nd-8th level $9.89 \times 10^5\ kg$ • 9th level $1.07 \times 10^6\ kg$		Restraints: Column splices are at 1.83 m w.r.t. beam-to-column joint; Columns pinned at base; Structure laterally restrained at 1st level.	

Fig. 5 – Left: Nine-story moment-resisting steel frame designed for the SAC Phase II Project coupled with a stepping rocking wall equipped with dampers at its pivoting points. Right: Geometric and physical characteristics pertinent to the nine-story SAC building.

medium-rise buildings designed for the greater area of Los Angeles, California. The building's dimensions and structural information is shown in Fig. 5. The nonlinear behavior of the yielding SDOF spring in MATLAB is matched with the pushover analysis results of 9-story building from OpenSees, as it shown in [24].

Fig. 6 compares response histories computed with OpenSees at mid-height of the 9-story SAC steel building coupled with a damped rocking wall with the solutions obtained with MATLAB for the SDOF idealization shown in Fig 1. In this figure, Comparison of the displacement time histories at mid-height of the nine-story building coupled with a damped rocking wall (hysteretic damping (top) and viscous damping (middle)) com-

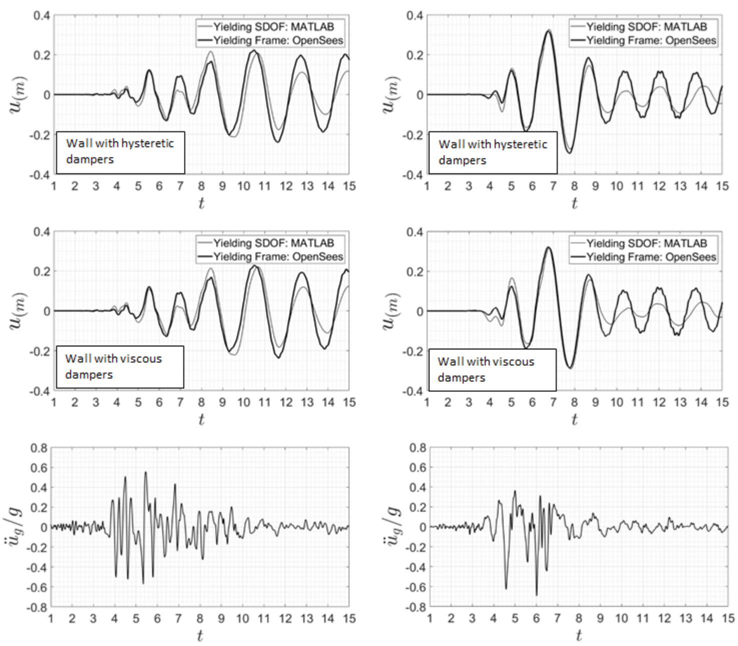

Fig. 6 – Comparison of the displacement time histories at mid-height of the nine-story building coupled with a damped rocking wall (hysteretic damping (top) and viscous damping (middle)) computed with OpenSees to the displacement time-histories of the SDOF idealization with MATLAB, when excited with the 1994 Newhall/360, Northridge, California (left) and the 1995 Takarazuka/000, Kobe, Japan (right) ground motions.

puted with OpenSees to the displacement time-histories of the SDOF idealization in Fig. 1 with MATLAB, when excited with the 1994 Newhall/360, Northridge, California (left) and the 1995 Takarazuka/000, Kobe, Japan (right) ground motions. The damping properties is chosen similar to the one that has been used in the stepping pier of the South Rangitikei Rail Bridge in New Zealand is used [3, 36, 37, 41] (similar to the previous step). The top plots are when the stepping rocking wall equipped with hysteretic dampers and the middle plots are when it is equipped with viscous dampers at its pivoting points. The comparison of the OpenSees and Matlab solutions are in good agreement–in particular for the peak-response values and supports the use of the SDOF idealization introduced in Fig 1.

5. Earthquake Spectra of a Yielding Oscillator Coupled with a Stepping Rocking Wall with Supplemental Damping

In this section, equations of motion (19) and (20) are used to generate inelastic response spectra. Fig. (7) plots displacement spectra of a yielding SDOF oscillator coupled with a stepping rocking wall with supplemental zero-length (left) and finite length (with $l/h = 0.2$ and $d/b = 0.1$) (right plots) equipped with linear viscous and hysteretic dampers when excited by the three different ground motions which labeled each accordingly.

First observation is that use of dampers are effective way of reducing maximum deformation in the coupled system and more damping leads to smaller deformations. Also, in some cases like in the case of hysteretic damper under 2011 REHS, Christchurch, New Zealand ground motion, damped system maximum response exceeds the undamped yielding oscillator coupled with stepping wall system, which shows that the effectiveness of hysteretic supplemental damping in suppressing the rocking response depends strongly on the kinematic

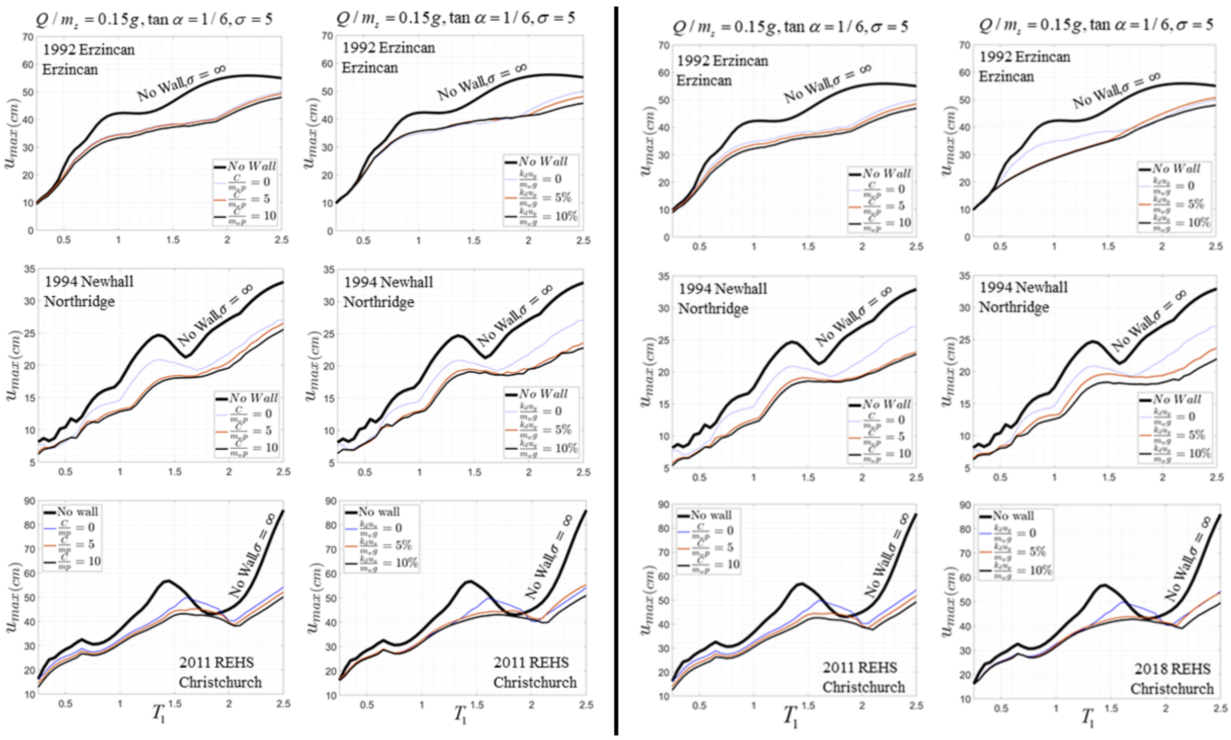

Zero-length Dampers

Dampers with $l/h = 0.2$ and $d/b = 0.1$

Fig. 7 – Peak response of SDOF yielding oscillator coupled with a stepping wall with slenderness $\tan\alpha = 1/6$ with zero-length (left plots) and finite length (with $l/h = 0.2$ and $d/b = 0.1$) (right plots) supplemental linear-viscous or hysteretic dampers, when excited by the three strong ground motions.

characteristics of the ground motion. Whenever the damped response exceeds that undamped response, the exceedance is marginal and in most cases the damped response is lower than the undamped response.

There are several situations where it is suitable to place the supplemental energy dissipation devices with a distance from the sides of a rocking wall. In this cases two additional parameters appear in the analysis, the distance d of the connection of the dissipation device from the pivoting point and the length, l of the dissipation device. Fig. 7 (right) plots maximum response diagrams for yielding oscillator coupled with rocking wall with slenderness $\tan\alpha = 1/6$ with finite-length supplemental viscous/hysteretic dampers with $l/h = 0.2$ and $d/b = 0.1$ and normalized damping constant $\frac{C}{m_w p} = 5$ and 10. In Fig. 7 (right) similar trends as those discussed for the corresponding Fig. 7 are observed; while the additional lever arm $d = 0.1b$ appears to have marginal effect on the peak response in particular for taller walls.

6. Conclusions

This paper investigates the inelastic response of a yielding structure coupled with a damped rocking wall. The full nonlinear equations of motion were derived, and the dependability of the one-degree-of-freedom idealization is validated against the nonlinear time-history response analysis of the 9-story SAC steel building.

The SDOF idealization presented in this paper compares satisfactory with finite-element analysis of a multi-story building coupled with a damped stepping rocking wall; therefore, the SDOF idealization can be used with confidence for preliminary analysis and design.

The study also shows that in most cases, use of dampers are effective way of reducing maximum deformation in the coupled system; while the additional lever arm for the dampers appears to have marginal effect on the peak response, in particular for taller walls.

References

[1] Paulay T (1969), The coupling of reinforced concrete shear walls, in: *The Fourth World Conference on Earthquake Engineering, Santiago, Chile.*

[2] Fintel M (1975), Ductile shear walls in earthquake-resistant multistory buildings, in: *Wind and Seismic Effects: Proceedings of the Seventh Joint Panel Conference of the US-Japan Cooperative Program in Natural Resources, Tokyo, Japan*, volume 470, US Department of Commerce, National Bureau of Standards, page 33.

[3] Kelly JM, Skinner R, and Heine A (1972), Mechanisms of energy absorption in special devices for use in earthquake resistant structures, *Bulletin of NZ Society for Earthquake Engineering*, **5**(3):63–88.

[4] Priestley MN (1991), Overview of presss research program, *PCI journal*, **36**(4):50–57.

[5] Nakaki SD, Stanton JF, and Sritharan S (1999), An overview of the presss five-story precast test building, *PCI journal*, **44**(2).

[6] Priestley MN, Sritharan S, Conley JR, and Pampanin S (1999), Preliminary results and conclusions from the presss five-story precast concrete test building, *PCI journal*, **44**(6):42–67.

[7] Kurama Y, Sause R, Pessiki S, and Lu LW (1999), Lateral load behavior and seismic design of unbonded post-tensioned precast concrete walls, *Structural Journal*, **96**(4):622–632.

[8] Kurama YC, Sause R, Pessiki S, and Lu LW (2002), Seismic response evaluation of unbonded post-tensioned precast walls, *Structural Journal*, **99**(5):641–651.

[9] Beck JL and Skinner R (1972), *The seismic response of a proposed reinforced concrete railway viaduct*, Report 369, Physics and engineering Laboratory DSIR, Report No 369.

[10] Beck JL and Skinner R (1974), The seismic response of a reinforced concrete bridge pier designed to step, *Earthquake Engineering & Structural Dynamics*, **2**(4):343–358.

[11] Makris N (2014), A half-century of rocking isolation, *Earthquakes and Structures*, **7**(6):1187–1221.

[12] Ajrab JJ, Pekcan G, and Mander JB (2004), Rocking wall-frame structures with supplemental tendon systems, *Journal of Structural Engineering*, **130**(6):895–903.

[13] Filiatrault A, Restrepo J, and Christopoulos C (2004), Development of self-centering earthquake resisting systems, in: *13th World Conference on Earthquake Engineering,Vancouver, Canada.*

[14] Holden T, Restrepo J, and Mander JB (2003), Seismic performance of precast reinforced and prestressed concrete walls, *Journal of Structural Engineering*, **129**(3):286–296.

[15] Lu Y (2005), Inelastic behaviour of rc wall-frame with a rocking wall and its analysis incorporating 3-d effect, *The Structural Design of Tall and Special Buildings*, **14**(1):15–35.

[16] Alavi B and Krawinkler H (2004), Strengthening of moment-resisting frame structures against near-fault ground motion effects, *Earthquake Engineering & Structural Dynamics*, **33**(6):707–722.

[17] Nicknam A and Filiatrault A (2014), Numerical evaluation of seismic response of buildings equipped with propped rocking wall systems, in: *10th U.S. National Conference on Earthquake Engineering, Anchorage, Alaska*.

[18] Toranzo L, Restrepo J, Mander J, and Carr A (2009), Shake-table tests of confined-masonry rocking walls with supplementary hysteretic damping, *Journal of Earthquake Engineering*, **13**(6):882–898.

[19] Wada A, Qu Z, Motoyui S, and Sakata H (2011), Seismic retrofit of existing src frames using rocking walls and steel dampers, *Frontiers of Architecture and Civil Engineering in China*, **5**(3):259–266.

[20] Qu Z, Wada A, Motoyui S, Sakata H, and Kishiki S (2012), Pin-supported walls for enhancing the seismic performance of building structures, *Earthquake Engineering & Structural Dynamics*, **41**(14):2075–2091.

[21] Makris N and Aghagholizadeh M (2017), The dynamics of an elastic structure coupled with a rocking wall, *Earthquake Engineering & Structural Dynamics*, **46**(6):945–962.

[22] Makris N and Aghagholizadeh M (2017), Earthquake protection of a yielding frame with a rocking wall, in: *International Workshop on Performance-Based Seismic Design of Structures (Resilience, Robustness), Shanghai, China*.

[23] Aghagholizadeh M and Makris N (2017), Seismic response of a yielding structure coupled with a rocking wall, *Journal of Structural Engineering*, **144**(2):04017196.

[24] Aghagholizadeh M and Makris N (2018), Earthquake response analysis of yielding structures coupled with vertically restrained rocking walls, *Earthquake engineering & structural dynamics*, **47**(15):2965–2984.

[25] Constantinou MC, Soong TT, and Dargush GF (1998), *Passive energy dissipation systems for structural design and retrofit*, Report, Multidiciplinary Center for Dearthquake Engineering Research.

[26] Symans M, Charney F, Whittaker A, Constantinou M, Kircher C, Johnson M, and McNamara R (2008), Energy dissipation systems for seismic applications: current practice and recent developments, *J. Struct. Eng.*, **134**(1):3–21.

[27] Wada A, Saeki E, Takeuchi T, and Watanabe A (1989), *Development of unbonded brace*, Report 115, Nippon Steel.

[28] Chang S and Makris N (2000), Effect of various energy dissipation mechanisms in supressing structural response, in: *12th World Conference on Earthquake Engineering, Auckland, New Zealand*.

[29] Black CJ, Aiken ID, and Makris N (2002), *Component testing, stability analysis, and characterization of buckling-restrained unbonded braces (TM)*, Report PEER 2002/08, Pacific Earthquake Engineering Research Center.

[30] Black CJ, Makris N, and Aiken ID (2004), Component testing, seismic evaluation and characterization of buckling-restrained braces, *Journal of Structural Engineering*, **130**(6):880–894.

[31] Bouc R (1967), Forced vibration of mechanical systems with hysteresis, in: *Fourth conference on non-linear oscillation, Prague, Czechoslovakia*.

[32] Wen YK (1976), Method for random vibration of hysteretic systems, *Journal of the engineering mechanics division*, **102**(2).

[33] Makris N and Aghagholizadeh M (2019), Effect of supplemental hysteretic and viscous damping on rocking response of free-standing columns, *Journal of Engineering Mechanics*, **145**(5):04019028.

[34] Kunnath SK, Mander JB, and Fang L (1997), Parameter identification for degrading and pinched hysteretic structural concrete systems, *Engineering Structures*, **19**(3):224–232.

[35] Goda K, Hong H, and Lee C (2009), Probabilistic characteristics of seismic ductility demand of sdof systems with bouc-wen hysteretic behavior, *Journal of Earthquake Engineering*, **13**(5):600–622.

[36] Skinner R, Kelly J, and Heine A (1974), Hysteretic dampers for earthquake-resistant structures, *Earthquake Engineering & Structural Dynamics*, **3**(3):287–296.

[37] Skinner R, Tyler R, Heine A, and Robinson W (1980), Hysteretic dampers for the protection of structures from earthquakes, *Bulletin of New Zealand National Society of Earthquake Engineering*, **13**(1):22–36.

[38] SAC Joint Venture (2000), Recommended seismic design criteria for new steel moment-frame buildings: Program to reduce the earthquake hazards of steel moment frame structures.

[39] Chopra AK and Goel RK (2002), A modal pushover analysis procedure for estimating seismic demands for buildings, *Earthquake Engineering & Structural Dynamics*, **31**(3):561–582.

[40] Aghagholizadeh M (2018), *Seismic Response of Moment Resisting Frames Coupled with Rocking Walls*, Ph.D. thesis, University of Central Florida.

[41] Blakeley WH, Charlesn AW, Hitchcock HC, M ML, Priestley MN, Sharpe RD, and Skinner R (1979), Recommendations for the design and construction of base isolated structures, *Bulletin of The NZ National Society for Earthquake Engineering*, **12**(2).

